Frequency-domain interferometer for measuring the phase and amplitude of a femtosecond pulse probing a laser-produced plasma

J. P. Geindre, P. Audebert, A. Rousse, F. Falliès, and J. C. Gauthier

Laboratoire pour l'Utilisation des Lasers Intenses, Ecole Polytechnique, 91128 Palaiseau, France

A. Mysyrowicz, A. Dos Santos, G. Hamoniaux, and A. Antonetti

Laboratoire d'Optique Appliquée, ENSTA, 91120 Palaiseau, France

Received June 8, 1994

A frequency-domain interferometer for probing the variations of the dielectric constant of a plasma with sub-100-fs temporal resolution and $\lambda/2000$ phase resolution is described. Imaging the plasma on the entrance slit of a spectrograph provides spatial resolution along a diameter of the focal spot. The technique is used to map out the expansion of the critical density surface of a femtosecond laser-produced plasma with subnanometer spatial resolution along the laser axis.

Since the development of ultrashort-pulse laser-interaction experiments on solid targets, the problem of the determination of the spatial scale length of the electron density gradient in hydrodynamically expanding plasmas has been difficult to solve.[1,2] Laser energy absorption mechanisms in the ultrafast regime depend critically[3,4] on the gradient scale length L, which has been shown by hydrodynamic simulations[5,6] to be much smaller than the laser wavelength λ ($L/\lambda \ll 1$). Femtosecond reflectivity imaging[7] and Schlieren measurements[8] permit only micrometer spatial resolution on the position of the expanding plasma surface. Other techniques involve the measurement of the absorption[9] or of the reflectivity of a probe pulse as a function of the incidence angle and of the polarization angle.[10,11] The gradient scale length and expansion velocities are then indirectly deduced by comparison with simulations. A more direct determination of the velocity of the critical density surface perturbed by laser ponderomotive force has been obtained from the Doppler shift of a reflected probe beam.[12] Recently, femtosecond time-resolved measurements of the phase change of a probe pulse by spectral blue shifting[13] and second-harmonic generation[14] have been reported. This has given access to the ionization dynamics of the plasma during the pump pulse and to its subsequent hydrodynamic expansion. These techniques give little or no information on the variation of the measured quantities along the focal spot diameter. However, spatial resolution in the radial direction can give access, in one shot, to the laser intensity variation of the measured parameters.

In this Letter we demonstrate a frequency-domain interferometer that permits the measurement of both the amplitude and the phase shift difference induced by the index of refraction of the plasma between a pair of femtosecond probe pulses with simultaneously high spatial and temporal resolution in two dimensions. Frequency-domain interferometry was described previously to phase lock a pair of femtosecond pulses[15] and to probe induce phase modulation in absorptive materials.[16] Our interferometer uses a similar design with the major addition of object imaging along a direction perpendicular to the spectral dispersion axis of the spectrograph. This permits one-dimensional spatial resolution along the diameter of the laser-producing pump focal spot.

The interferometer principle is shown in Fig. 1. The main laser system provides a high-intensity pump pulse and a much shorter duration auxiliary pulse that can be delayed arbitrarily in time. The auxiliary pulse is further divided into two arms of a Michelson interferometer to generate the final probe and reference pulses, which are separated temporally by adjustment of one of the arm lengths. We note that this kind of interferometer is highly stable against thermal and vibration fluctuations because the path difference between the probe and the reference beams is only the two short arms of the Michelson interferometer.

In frequency-domain interferometry, the reference beam and the probe beam are carefully aligned along the same axis so that they follow exactly the same optical path. In the basic configuration, the reference pulse irradiates the target surface before the plasma-producing pump pulse, and the second pulse probes the plasma after the pump (see Fig. 1). The focal spot size of the probe and reference beams is several times larger than the pump focal spot size to permit uniform illumination of the region under test. The plasma illuminated by the twin probe pulses is imaged upon the entrance slit of an imaging spectrograph. The imaging lens provides spatial resolution along a diameter of the pump focal spot, perpendicular to the plane of incidence. In our setup the magnification of the imaging system is $\sim$100. The resolution of the complete system (imaging system plus spectrograph plus camera) is $\sim$1 μm. The temporally separated pulses can interfere because of

0146-9592/94/231997-03$6.00/0

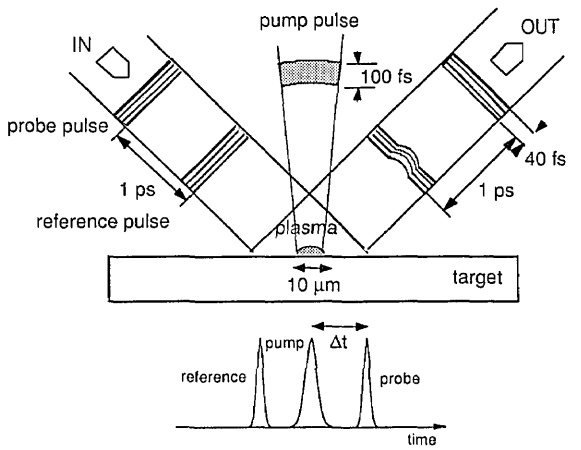

Fig. 1. Frequency-domain interferometer principle. Typical dimensions and times are indicated. The probe and reference pulses interfere after passing through a grating pulse stretcher.

the dispersion of the spectrograph grating, which, acting as pulse stretcher, broadens the pulses to make them overlap in time. The interference pattern is recorded by a CCD camera.

The theory of operation of the interferometer is straightforward.[16] We mention it briefly to discuss the ultimate sensitivity of the instrument. Let us consider a point along the entrance slit of the spectrograph that is the image of a point along the diameter perpendicular to the plane of incidence of the probe beams. We assume that the probe pulses are Fourier-transform limited so that their bandwidth and duration are related by $\Delta\omega\Delta t_p \approx 2\pi$. The expression for the reference pulse field is $\mathbf{E}_0(t) = E_0(t)\exp(i\omega_0 t)$. After being reflected from the plasma surface, the probe pulse delayed by Δt from the reference pulse undergoes a phase change $\Delta\Phi$, and its intensity is reduced by a factor R (an effective reflection coefficient). The probe pulse field is now $\mathbf{E}_1(t) = E_0(t - \Delta t)\sqrt{R}\,\exp\{i[\omega_0(t - \Delta t) + \Delta\Phi]\}$. The intensity measured by the camera is the square of the Fourier transform of the sum of these two fields:

$$I(\omega) = I_0(\omega)[1 + R + 2\sqrt{R}\,\cos(\omega\Delta t + \Delta\Phi)]. \quad (1)$$

The Fourier transform of the twin probe pulses presents a spectral envelope that is identical to the spectrum $I_0(\omega)$ of a single probe pulse modulated by a cosine function, from which we can obtain simultaneously the reflection coefficient and the phase difference from the amplitude changes and peak shifts of the fringes, respectively. The spatial wavelength of the fringes is given by $(2\pi/\Delta t)\delta x/\delta\omega$, where $\delta x/\delta\omega$ is the spectral dispersion of the grating. The complete fringe system along the dispersion axis gives information on one single point along the diameter of the pump pulse focal spot. Thus the signal-to-noise ratio is increased proportionally to the number of points along a line of the detectors and the results are largely insensitive to the local defects of the detector.

To extract the phase information from the spectral domain, we calculate the inverse Fourier transform of $I(\omega)$:

$$\mathrm{TF}[I(\omega)](t') = (1 + R)G(t') + \sqrt{R}\,\exp(i\Delta\Phi)G(t' - \Delta t) - \sqrt{R}\,\exp(-i\Delta\Phi)G(t' + \Delta t), \quad (2)$$

where the inverse Fourier transform of the original probe pulses is $G(t')$. For $\Delta t \gg \Delta t_p$, the lateral peaks at $t' \pm \Delta t$ contain the phase information. We note that, when $\Delta\Phi$ and R vary during the time duration of the probe pulse, it can be shown that the measurement gives the temporal average of the phase weighted by the amplitude of the reflected pulses when the phase variation is smaller than $\pi/2$.

The CCD noise and digital resolution are the most important sources of phase noise. To the signal $I(\omega)$, this adds a background noise $B(\omega)$. This noise affects only the spatial resolution perpendicular to the target. For a camera with N pixels along a line, it can be shown that the standard deviation of the phase noise is

$$\sigma(\Delta\Phi) = \sqrt{N}\,\sigma(B)/\sqrt{2R}\,G(0), \qquad \sigma^2(B) = \langle B(\omega)^2\rangle.$$

The phase noise does not depend on the number of fringes; it is proportional to the signal-to-noise ratio of the camera. In our measurements we use a standard CCD video camera with 400 pixels digitized over 8 bits. For a useful spectrum covering 200 pixels FWHM with an average reading of 100, we have $G(0) = 5000$ and thus $\sigma(\Delta\Phi) = 2.8 \times 10^{-3}\,\sigma(B)$ rad. Because a calibration shot also is needed (see below), the final fluctuation is $\sigma(\Delta\Phi) = 0.004\,\sigma(B)$. Experimentally, we have obtained $\sigma(\Delta\Phi) = 0.006$ rad, corresponding to a fringe shift of 10^{-3} fringe. Measuring a fringe shift of 10^{-3} fringe corresponds to measuring a spatial variation of 0.01 pixel, or approximately 0.2 μm on the spectrograph slit. With this degree of accuracy, the defects of the slit should be taken into account by a calibration shot, and the thermal and mechanical stability of the detector systems should be ensured between the calibration and the measurement shot.

Because of the relation between the number of fringes and the time separation between the twin probe pulses, this separation cannot be made arbitrarily large. Accordingly, two modes of operation are possible. For a time delay between the pump and the probe pulses shorter than the separation of the probe pulses, the measurement gives the phase difference between the unperturbed target and the plasma. We measure the phase variations of the probe induced by plasma heating during the laser pulse, and, at later times when the phase shift is governed by the expansion velocity of the critical surface, we monitor—in two dimensions—the position of the critical surface where the electron density is equal to the critical density $n_c = 10^{21}(1.06/\lambda)^2$. This is the absolute mode. In the second mode, for delay times larger than the separation of the probe and the reference pulses, the measurement probes the index-of-refraction change between two different times in the expansion of the plasma. This is the relative mode. In reflection measurements, we thus obtain directly the expansion velocity of the critical density surface.

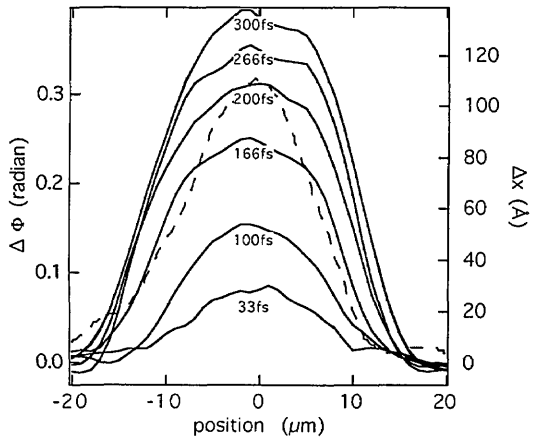

Fig. 2. Space- and time-resolved phase measurement of an aluminum plasma at 3×10^{15} W/cm^2 irradiance. Phases have been converted to positions along the normal to the target surface on the right-hand scale. The radial laser intensity shape (in linear arbitrary units) is given by the dashed curve.

The capability of the technique has been demonstrated by measurement of the phase shift induced by an aluminum target irradiated by a 77-fs laser pulse at an irradiance of 3×10^{15} W/cm^2. The pump pulse is provided by a colliding-pulse mode-locked oscillator followed by a series of dye amplifiers (620-nm wavelength) pumped at a repetition rate of 10 Hz by a diode-injected, frequency-doubled, Q-switched Nd:YAG laser. A synchronized 40-fs probe pulse at 590 nm is also available.[8] The incidence angle of the twin probe pulses, separated by 390 fs, is 45° with respect to the target normal, and the pulses are polarized perpendicularly to the plane of incidence (S polarization). The pump laser can be delayed with respect to the probe pulse in the range 0–390 fs (absolute mode) and with respect to the reference pulse in the range 390–3000 fs (relative mode). Zero time delay is obtained when the probe and the pump pulses coincide in time.

An interferogram was obtained for each delay between the pump and the probes. The inverse Fourier transform was calculated on line from the digitized image. Figure 2 shows the measured phase shift as a function of time and space along a diameter of the focal spot. Competing phase contributions of probe beam propagation in the underdense plasma, reflection and absorption near the critical surface, and expansion of the plasma (Doppler phase) influence the measured phase shift at different times. Hydrodynamic simulations[6] show that, at times longer than 200 fs after the maximum of the pump pulse, the contribution to the phase of the critical surface expansion dominates. We then can relate the phase shift directly to the position of the critical surface (see Fig. 2), which acts as a moving mirror.

This new Fourier-domain interferometer allows us to measure the amplitude and phase variations of a probe pulse interacting with a plasma. The temporal resolution is limited by the duration of the probe pulse. The spatial resolution along the diameter of the plasma is limited by the optical imaging device. The ultimate sensitivity in the phase measurement is of the order of $\lambda/2000$. This instrument can provide radial resolution to study the laser intensity variations of ponderomotive electron density gradient steepening.[12,17] It can be used in transmission to probe the carrier dynamics in transparent materials.[18] It also is well adapted to perform studies of high-intensity laser beam propagation in gases in which small modulations of electron density in a plasma wave have to be detected. This is important for x-ray laser research[19] and electron acceleration by laser wake fields.[20]

We acknowledge very helpful discussions with A. Migus and J. P. Chambaret.

References

1. R. Fedosejevs, R. Ottmann, R. Sigel, G. Kühnle, S. Szatmari, and F. P. Schäfer, Appl. Phys. B **50,** 79 (1990).
2. U. Teubner, J. Bergmann, B. v. Wonterghem, F. P. Schäfer, and R. Sauerbrey, Phys. Rev. Lett. **70,** 794 (1993).
3. F. Brunel, Phys. Rev. Lett. **59,** 52 (1987).
4. P. Gibbon and A. R. Bell, Phys. Rev. Lett. **68,** 1535 (1992).
5. M. Rosen, Proc. Soc. Photo-Opt. Instrum. Eng. **1229,** 160 (1990).
6. R. C. Mancini, P. Audebert, J. P. Geindre, A. Rousse, F. Falliès, J. C. Gauthier, A. Mysyrowicz, J. P. Chambaret, and A. Antonetti, J. Phys. B **27,** 1671 (1994).
7. M. C. Downer, R. L. Fork, and C. V. Shank, J. Opt. Soc. Am. B **2,** 595 (1985).
8. R. Benattar, J. P. Geindre, P. Audebert, J. C. Gauthier, J. P. Chambaret, A. Mysyrowicz, and A. Antonetti, Opt. Commun. **88,** 376 (1992).
9. O. L. Landen, D. G. Stearn, and E. M. Campbell, Phys. Rev. Lett. **63,** 1475 (1989).
10. H. M. Milchberg, R. R. Freeman, and S. C. Davey, Phys. Rev. Lett. **61,** 2364 (1988).
11. X. Y. Wang and M. C. Downer, Opt. Lett. **17,** 1450 (1992).
12. X. Liu and D. Umstadter, Phys. Rev. Lett. **69,** 1935 (1992).
13. W. M. Wood, C. W. Siders, and M. C. Downer, Phys. Rev. Lett. **67,** 3523 (1991).
14. D. van der Linde, H. Schultz, T. Engers, and H. Schüler, IEEE J. Quantum Electron. **28,** 2388 (1992).
15. N. F. Scherer, R. J. Carlson, A. Matro, M. Du, A. Ruggiero, V. Romero-Rochin, J. A. Cina, G. R. Fleming, and S. A. Rice, J. Chem. Phys. **95,** 1487 (1991).
16. E. Tokunaga, A. Terasaki, and T. Kobayashi, Opt. Lett. **17,** 1131 (1992).
17. S. C. Wilks, W. L. Kruer, M. Tabak, and A. B. Langdon, Phys. Rev. Lett. **69,** 1383 (1992).
18. P. Audebert, J. P. Geindre, J. C. Gauthier, P. Daguzan, S. Guizard, P. Martin, and G. Petite, in *Ultrafast Phenomena,* Vol. 7 of 1994 OSA Technical Digest Series (Optical Society of America, Washington, D.C., 1994), paper PDP1.
19. D. C. Eder, P. Amendt, and S. C. Wilks, Phys. Rev. A **45,** 6761 (1992).
20. P. Sprangle and E. Esarey, Phys. Fluids B **4,** 2241 (1992).